Image Cover Sheet

92-00196

CLASSIFICATION	SYSTEM NUMBER
UNCLASSIFIED	103097

TITLE

EIGENVECTOR WEIGHTING AS AN ADAPTIVE ARRAY INTERFERENCE CANCELLATION TECHNIQUE

System Number:

Patron Number:

Requester:

Notes: paper 16

DSIS Use only:

Deliver to: FF

EIGENVECTOR WEIGHTING AS AN ADAPTIVE ARRAY INTERFERENCE CANCELLATION TECHNIQUE

R.W. Jenkins and K.W. Moreland
Communications Research Centre
Box 11490, Station H
Ottawa, Canada K2H 8S2

SUMMARY

Adaptive antenna techniques normally make use of known properties of the desired signal, such as its direction or an embedded code, to distinguish it from interference. When this is not possible, algorithms such as power ratio inversion or Gram-Schmidt are used. These techniques tend to invert the relative powers of signals arriving at the array, and thus are effective when the interference is substantially stronger than the desired signal. However, when signal levels are close, such techniques fail. This paper presents analytic and modelling studies of the eigenvector weighting technique. It is shown that this technique performs substantially better than power ratio inversion techniques. Like the power ratio inversion methods, eigenvector weighting is most effective when there is a large separation in signal powers. However, even when the signals are close in power, satisfactory cancellation can be achieved with eigenvector weighting for a large fraction of cases. The actual performance depends on array geometry and number of elements.

INTRODUCTION

In a crowded, possibly hostile, radio environment, communication is threatened by interference due to other users or enemy jammers. Many-user nets require a means of discriminating between concurrent users. Adaptive antenna arrays provide spatial discrimination against interference, and a means of separating the signals from multiple users in a net. These arrays normally employ techniques which use known features of a desired signal, such as a predetermined embedded code or a known direction, in order to distinguish it from other signals.

Predetermined identification techniques are not appropriate for some communications signals. Strategies which may be used in such cases include the power ratio inversion algorithm [1] and the Gram-Schmidt orthogonalization approach [2]. These techniques tend to invert the relative powers of signals incident on the array, yielding a desired signal at the output which is as much above the co-channel interference level as its input counterpart is below the interference.

Eigenvector weighting has been proposed as a means of separating independent incident signals [3]. Using eigenvectors of the covariance matrix of the input signals as weights to transform the array inputs yields a set of uncorrelated output signals. This lack of correlation is a property also of the independent incident signals, and it has been suggested that the output signals produced by eigenvector transformation consist mainly of the independent incident signals. There is a fallacy in this reasoning. There exist linear combinations of the incident signals which are uncorrelated. There are also other transformations such as Gram-Schmidt orthogonalization which cause the outputs to be uncorrelated. Nonetheless, modelling and simulation studies [3,4] indicate good performance for the eigenvector technique when the signals of interest are well separated in power.

This paper presents analytic and modelling studies of the eigenvector technique. Its performance relative to power ratio inversion is considered.

SIGNAL FORMULATION

A complex baseband formulation is used in this analysis. Column vectors are indicated by $\tilde{}$, matrices, by bold type, and the complex conjugate, transpose, and conjugate transpose operations, by *, ^{T}, and ^{H}, respectively.

Consider m independent signals with baseband time dependence $s_j(t)$, j=1,m, incident on an n-element array. Let g_{ij} be the complex gain of the ith element of the array to the jth signal. The resultant signal at element i is given by

$$x_i = \sum_{j=1}^{m} g_{ij} s_j + n_i \qquad (1)$$

where n_i is the noise present on the ith channel. The array response vector $\tilde{g}_j$ to the jth signal is defined as

$$\tilde{g}_j = [\, g_{1j},\ g_{2j},\ \text{--},\ g_{nj}]^T \qquad (2)$$

and the n x m array response matrix **G** to the collection of signals, is likewise defined as

$$\mathbf{G} = \begin{bmatrix} g_{11} \cdots g_{1j} \cdots g_{1m} \\ \cdots \cdots \cdots \cdots \cdots \\ g_{i1} \cdots g_{ij} \cdots g_{im} \\ \cdots \cdots \cdots \cdots \cdots \\ g_{n1} \cdots g_{nj} \cdots g_{nm} \end{bmatrix} = [\tilde{g}_1, \tilde{g}_2, \cdots, \tilde{g}_m] \qquad (3)$$

Using the array response matrix, (1) can be expressed in vector form as

$$\tilde{x} = \mathbf{G}\,\tilde{s} + \tilde{n}\,, \text{ where} \qquad (4)$$

$\tilde{x} = [x_1, x_2, \cdots, x_n]^T$, $\tilde{s} = [s_1, s_2, \cdots, s_m]^T$, and $\tilde{n} = [n_1, n_2, \cdots, n_n]^T$ are the array input, signal, and noise vectors respectively.

The covariance matrix **R** of the input signals is given by

$$\mathbf{R} = \begin{bmatrix} \langle x_1 x_1^* \rangle & \langle x_1 x_2^* \rangle & \cdots & \langle x_1 x_n^* \rangle \\ \langle x_2 x_1^* \rangle & \langle x_2 x_2^* \rangle & \cdots & \langle x_2 x_n^* \rangle \\ \cdots & \cdots & \cdots & \cdots \\ \langle x_n x_1^* \rangle & \langle x_n x_2^* \rangle & \cdots & \langle x_n x_n^* \rangle \end{bmatrix} = \langle \tilde{x}\,\tilde{x}^H \rangle \qquad (5)$$

where $\langle\ \rangle$ represents the statistical average, which is approximated in practice by a time average. The input signals s_j, j=1,m and channel noise signals n_i, i=1,n are assumed to be independent and thus non-correlating. Using (4) and (5), the covariance matrix can be written as

$$\mathbf{R} = \mathbf{G}\mathbf{P}\mathbf{G}^H + \mathbf{N} \qquad (6)$$

where $\mathbf{P} = \begin{bmatrix} P_1 & 0 & \cdots & 0 \\ 0 & P_2 & \cdots & 0 \\ \cdots & \cdots & \cdots & \cdots \\ 0 & 0 & \cdots & P_m \end{bmatrix}$ is the matrix of the signal powers $P_j = \langle s_j s_j^* \rangle$, and $\mathbf{N} = \begin{bmatrix} N_1 & 0 & \cdots & 0 \\ 0 & N_2 & \cdots & 0 \\ \cdots & \cdots & \cdots & \cdots \\ 0 & 0 & \cdots & N_n \end{bmatrix}$, the matrix of the channel noise powers $N_i = \langle n_i n_i^* \rangle$. In the subsequent analysis, the noise power is assumed to be independent of channel number, so that **N** may be written

$$\mathbf{N} = \sigma^2 \mathbf{I} \qquad (7)$$

where **I** is the n x n identity matrix, and σ^2 is the noise power per channel. Although the noise level may not be constant between channels in practice, this introduces little error provided the noise levels are much lower than the signal levels of interest.

EIGENVECTOR SEPARATION TECHNIQUE

In the eigenvector separation technique the eigenvectors of the covariance matrix **R** are used as weight vectors to transform the array input signals vector $\tilde{x}$ into an output vector $\tilde{y}$. If the technique is successful the components of $\tilde{y}$ should consist primarily of the separated independent signals s_j. The interference cancellation problem is then reduced to selecting the output channel which contains the desired signal.

Since **R** is a covariance matrix, it is Hermitian, its eigenvalues are real and non-negative, and its eigenvectors orthogonal [5]. Define $\mathbf{E} = [\tilde{e}_1, \tilde{e}_2, \cdots, \tilde{e}_n]$ as the matrix whose column vectors are the normalized eigenvectors $\tilde{e}_i$ of **R**, ordered according to the size of their corresponding eigenvalues λ_i, from largest to smallest. As the eigenvectors $\tilde{e}_i$ are normalized and orthogonal, **E** is a unitary matrix.

The eigenvector equation can be written

$$\mathbf{R}\mathbf{E} = \mathbf{E}\mathbf{\Lambda} \qquad (8)$$

where $\mathbf{\Lambda}$ is the diagonal matrix whose ith diagonal element is the eigenvalue λ_i corresponding to the eigenvector $\tilde{e}_i$. Since $\mathbf{E}^H = \mathbf{E}^{-1}$ for unitary matrices, premultiplying both sides of (8) by $\mathbf{E}^H$ yields

$$\mathbf{E}^H\mathbf{R}\mathbf{E} = \mathbf{\Lambda}\,. \qquad (9)$$

The eigenvectors are used as weights to transform the array input signals vector $\tilde{x}$,

$$y_i = \tilde{e}_i^H \tilde{x}\,, \text{ or } \tilde{y} = \mathbf{E}^H \tilde{x} \qquad (10)$$

where $\tilde{y} = [y_1, y_2, \cdots, y_n]^T$ is the vector of output signals. From equation 9 the covariance matrix $\mathbf{R}'$ of the output signals is the diagonal matrix of the eigenvalues,

$$\mathbf{R}' = \langle \tilde{y}\,\tilde{y}^H \rangle = \mathbf{E}^H \langle \tilde{x}\,\tilde{x}^H \rangle \mathbf{E} = \mathbf{E}^H\mathbf{R}\mathbf{E} = \mathbf{\Lambda} \qquad (11)$$

Equation 11 implies that the use of eigenvectors as weights yields a set of output signals y_i which are non-correlating.

In equation 6 the covariance matrix **R** was written as the sum of two matrices, one due to the signals, and the other due to noise:

$$\mathbf{R} = \mathbf{S} + \mathbf{N}, \text{ where } \mathbf{S} = \mathbf{G}\mathbf{P}\mathbf{G}^H \qquad (12)$$

If the array response vectors $\tilde{g}_j$ to the signals s_j, j=1,m, are independent, then **S** is of rank m and has m non-zero eigenvalues. **S** is Hermitian and its eigenvectors are orthogonal. Let $\tilde{u}_i$, i=1,m, be the normalized eigenvectors of **S** and γ_i be their corresponding eigenvalues. Since **N** is of the form $\sigma^2\mathbf{I}$ (equation 7),

$$\mathbf{R}\tilde{u}_i = (\gamma_i + \sigma^2)\tilde{u}_i \ . \qquad (13)$$

It is evident from (13) that the eigenvectors $\tilde{u}_i$ of **S** are also eigenvectors of **R**, and the eigenvalues of **R** are given by

$$\lambda_i = \gamma_i + \sigma^2 \qquad (14)$$

Therefore $\tilde{u}_i$ can be replaced by $\tilde{e}_i$, i=1,m, and expressed as columns of the matrix $\mathbf{E}_S = [\tilde{e}_1, \tilde{e}_2, \text{- -}, \tilde{e}_m]$, ordered as before from largest to smallest. The eigenvectors $\mathbf{E}_S$ are determined by the signals and span the signal subspace of **R**.

In addition to these orthonormal vectors, an arbitrary set of n-m orthonormal vectors $\tilde{e}_j$, j=m+1,n, can be chosen from the remaining orthogonal subspace of **R**. These vectors are transformed by **S** into the null vector, and are eigenvectors of **R** corresponding to the common eigenvalue σ^2 :

$$\mathbf{R}\tilde{e}_j = (\mathbf{S} + \mathbf{N})\,\tilde{e}_j = \mathbf{N}\tilde{e}_j = \sigma^2\tilde{e}_j \qquad (15)$$

The matrix of these remaining eigenvectors is denoted by

$$\mathbf{E}_N = [\tilde{e}_{m+1}, \tilde{e}_{m+2}, \text{- - }, \tilde{e}_n] \qquad (16)$$

The total set of eigenvectors is then represented by the columns of the matrix

$$\mathbf{E} = [\mathbf{E}_S, \mathbf{E}_N] \qquad (17)$$

where $\mathbf{E}_S$ spans the signal subspace and $\mathbf{E}_N$ spans the noise subspace of **R**.

From equations 11, 14, and 15 the output correlation matrix $\langle \tilde{y}\,\tilde{y}^H \rangle$ the output signals are noncorrelating, with powers given by the diagonal elements of $\langle \tilde{y}\,\tilde{y}^H \rangle$ according to

$$P_i(\text{out}) = \langle y_i\, y_i^* \rangle = \begin{cases} \gamma_i + \sigma^2 & \text{for i=1 to m} \\ \sigma^2 & \text{for i=m+1 to n} \end{cases} \qquad (18)$$

Consequently, under eigenvector weighting, the first m output channels contain the signals plus noise while the last n-m contain noise only.

CONDITIONS FOR PERFECT SIGNAL SEPARATION

One is tempted to suggest that since the original independent signals are non-correlating, the eigenvector transformation has separated the array input signals into the original signals. While this is not true in general, it is enlightening to explore the conditions under which perfect signal separation is achieved.

It is now shown that perfect separation of signals by the eigenvector technique occurs only if the array signal-response vectors are orthogonal.

From equations 4 and 10 the output signal $\tilde{y}$ can be expressed in terms of the input signals $\tilde{s}$ and noise $\tilde{n}$ by

$$\tilde{y} = \mathbf{E}^H\tilde{x} = \mathbf{E}^H\mathbf{G}\,\tilde{s} + \mathbf{E}^H\tilde{n} = \mathbf{A}\,\tilde{s} + \mathbf{E}^H\tilde{n} \qquad (19)$$

where $\mathbf{A} = \mathbf{E}^H\mathbf{G}$ is an n x m matrix having ijth component a_{ij}. The signal for the ith output channel is given by

$$y_i = \sum_{k=1}^{m} a_{ik}s_k + \text{noise term} \qquad (20)$$

Perfect signal separation means that each independent signal s_k is found in one and only one output channel. The signal ordering is arbitrary and can be chosen so that s_k appears in the kth channel, for k=1,m. This means, using (20), that the components of **A** can be written as $a_{ik} = a_i\,\delta_{ik}$, where δ_{ik} is the Kroenecker delta. Since $\mathbf{E}^H\,\mathbf{G} = \mathbf{A}$, and **E** is unitary, the array response matrix can be expressed as

$$\mathbf{G} = \mathbf{EA} = [\tilde{e}_1, \tilde{e}_2, \text{- -}, \tilde{e}_n]\begin{bmatrix} a_1 & 0 & .. & 0 \\ 0 & a_2 & .. & 0 \\ .. & .. & .. & .. \\ 0 & 0 & .. & a_m \\ 0 & 0 & .. & 0 \\ .. & .. & .. & .. \\ 0 & 0 & .. & 0 \end{bmatrix}$$

or,

$$\mathbf{G} = [\tilde{g}_1, \tilde{g}_2, \text{- -}, \tilde{g}_m]$$

$$= [a_1\tilde{e}_1, a_2\,\tilde{e}_2, \text{- -}, a_m\tilde{e}_m] \qquad (21)$$

Since the eigenvectors $\tilde{e}_j$ are orthonormal, the array response vectors $\tilde{g}_j$ are orthogonal.

The converse is also true (orthogonal response vectors implies that eigenvector weighting separates the signals perfectly), provided the signal-related eigenvalues are distinct. This is shown next.

If the array response vectors $\tilde{g}_j$ are orthogonal, they can be shown to be eigenvectors of **R** by postmultiplying (6) by $\tilde{g}_j$,

$$\mathbf{R}\tilde{g}_j = \mathbf{G}\mathbf{P}\mathbf{G}^H \tilde{g}_j + \mathbf{N}\tilde{g}_j = |\tilde{g}_j|^2 P_j \tilde{g}_j + \sigma^2 \tilde{g}_j = \lambda_j \tilde{g}_j \tag{22}$$

where $\lambda_j = |\tilde{g}_j|^2 P_j + \sigma^2$ is the corresponding eigenvalue of **R**. Since the signal eigenvalues λ_j are distinct, the corresponding normalized eigenvectors consist of the unique signal eigenvectors given by

$$\mathbf{E}_S = [\tilde{g}_1/|\tilde{g}_1|, \tilde{g}_2/|\tilde{g}_2|, \text{--}, \tilde{g}_m/|\tilde{g}_m|] \tag{23}$$

plus the orthogonal noise eigenvectors $\mathbf{E}_N = [\tilde{e}_{m+1}, \tilde{e}_{m+2}, \text{- -}, \tilde{e}_n]$. From (23), (17) and the orthogonality of **G** and $\mathbf{E}_N$, **A** can be written as

$$\mathbf{A} = \mathbf{E}^H\mathbf{G} = \begin{bmatrix} \mathbf{E}_S^H \\ \mathbf{E}_N^H \end{bmatrix}\mathbf{G} = \begin{bmatrix} |g_1| & 0 & .. & 0 \\ 0 & |g_2| & .. & 0 \\ .. & .. & .. & .. \\ 0 & 0 & .. & |g_m| \\ 0 & 0 & .. & 0 \\ .. & .. & .. & .. \\ 0 & 0 & .. & 0 \end{bmatrix} \tag{24}$$

Thus **A** has a quasi-diagonal form, which from (20) is equivalent to perfect signal separation at the output.

TWO-SIGNAL CASE

When only two signals (e.g., a communications signal and a single interfering signal) are incident on an array using eigenvector weighting, only the first two output channels will contain signal contributions (equation 18). The signals in these two channels are uncorrelated (equation 11). As will now be shown, this lack of correlation has interesting implications.

The output signals y_1, y_2 can be written in terms of the initial independent signals s_1, s_2 and channel noise n_k, k=1,n, as

$$y_i = a_{i1}s_1 + a_{i2}s_2 + \sum_{k=1}^{n} w_{ki}^* n_k, \quad i = 1,2 \tag{25}$$

where w_{ki}, k=1,n, are the weights $\tilde{w}_i$ used for the ith output channel. The non-correlation of outputs y_1 and y_2 can be expressed using (25) and the fact that the signals s_i and noise n_k do not correlate, as

$$\begin{aligned} 0 &= \langle y_1 y_2^* \rangle \\ &= a_{11}a_{21}^* P_1 + a_{12}a_{22}^* P_2 + \tilde{w}_1^H \tilde{w}_2 \sigma^2 \end{aligned} \tag{26}$$

P_1, P_2, and σ^2 are the signal and noise powers respectively. The eigenvector weights are orthogonal, making the last term of (26) zero. Equation 26 becomes

$$\frac{P_1}{P_2} = -\frac{a_{12}\,a_{22}^*}{a_{11}\,a_{21}^*} \tag{27}$$

From (25), the power due to the jth signal s_j in the ith output channel is given by

$$P_{ij}(i) = a_{ij}\,a_{ij}^* P_j \tag{28}$$

and the ratios of the powers of the signals s_1 and s_2 in the ith output channel, by

$$\frac{P_{1(i)}}{P_{2(i)}} = \frac{a_{i1}\,a_{i1}^*}{a_{i2}\,a_{i2}^*}\frac{P_1}{P_2} \tag{29}$$

By manipulating (27) and (29), it is seen that

$$\frac{P_{1(1)}}{P_{2(1)}} = \frac{P_{2(2)}}{P_{1(2)}} \tag{30}$$

Interpreting one of the signals as a desired signal and the other as interference, equation 30 states that the signal-to-interference ratio is inverted between the two output signal channels.

PERFORMANCE RELATIVE TO POWER RATIO INVERSION

The Gram-Schmidt weighting technique [2], like the eigenvector weighting technique, produces outputs signals which do not correlate. Equation 30 can be shown to apply to this technique as well, for low noise levels [6]. Since for the Gram-Schmidt technique, the first output channel is the same as the first input channel, the second output channel may be interpreted as inverting the relative powers of the two signals as seen by the first array element. The constrained matrix inversion technique can be shown to have a performance similar to that of the Gram-Schmidt method [2,6]. These two techniques thus have a performance similar to that of the power ratio inversion algorithm [1].

This section compares the performance of eigenvector weighting to that of the above-mentioned power-ratio-inverting techniques in separating two incoming signals. It is shown that for arrays with similar element antenna patterns, eigenvector weighting performs better than power ratio inversion for all signal directions, with power ratio inversion providing a greatest lower bound to the eigenvector performance.

It is noted that the array input $\tilde{x}$ of a number of signals s_i, i=1,m incident on an n-element array with common element pattern $g(\theta,\phi)$, where θ and ϕ represent signal arrival direction azimuth and elevation respectively, is the same as the array input of a number of signals $s_i' = g(\theta_i,\phi_i)s_i$, i=1,m, incident on an array of identical geometry and isotropic element patterns. Therefore the condition of identical element patterns may be replaced by the easier-to-handle condition of isotropic patterns.

From equation 4, the signal in the first eigenvector output channel is given by

$$y_1 = \tilde{e}_1^H \tilde{x} = \tilde{e}_1^H \mathbf{G} \tilde{s} + \tilde{e}_1^H \tilde{n}$$

$$= (\tilde{e}_1^H \tilde{g}_1)s_1 + (\tilde{e}_1^H \tilde{g}_2)s_2 + \tilde{e}_1^H \tilde{n} \qquad (31)$$

The first term on the right side of (31) is due to signal 1, the second, to signal 2, and the third, to noise. Therefore the ratio of signal powers in channel 1 is given for the eigenvector technique by

$$\left.\frac{P_{1(1)}}{P_{2(1)}}\right|_{eiv} = \frac{|\tilde{e}_1^H \tilde{g}_1|^2}{|\tilde{e}_1^H \tilde{g}_2|^2} \frac{P_1}{P_2} \qquad (32)$$

According to the ordering adopted in this paper, $P_1 \geq P_2$. This ordering, together with equations 30 and 32, implies that the eigenvector technique provides better signal separation than power ratio inversion when $|\tilde{e}_1^H \tilde{g}_1| > |\tilde{e}_1^H \tilde{g}_2|$, and when $|\tilde{e}_1^H \tilde{g}_1| = |\tilde{e}_1^H \tilde{g}_2|$, the signal separation provided by eigenvector weighting matches that of power ratio inversion. Therefore the problem, of proving that the performance of eigenvector weighting is everywhere better than that of power ratio inversion with power ratio inversion providing a greatest lower bound to eigenvector performance, is reduced to proving that

$$|\tilde{e}_1^H \tilde{g}_1| \geq |\tilde{e}_1^H \tilde{g}_2| \qquad (33)$$

everywhere with the equality being a limiting case.

The proof of (33) is of some length and is given in the Appendix.

COMPUTER-MODELLING

The eigenvector weighting technique was modelled on a PC using the MATLAB numeric computation package, for the case of a communications signal and a single jamming signal.

Except as noted, array element patterns were modelled as isotropic. The array response matrix $\mathbf{G} = [\tilde{g}_1, \tilde{g}_2]$ (equations 1-3) was calculated from a given array geometry and signal directions. The ideal covariance matrix $\mathbf{R}$ was then calculated from response matrix $\mathbf{G}$, together with given input signal powers P_1, P_2, and channel-independent noise power σ^2, using equations 6 and 7. From the ideal covariance matrix thus obtained, the normalized eigenvectors $\tilde{e}_k$, k=1,n, were computed, and ordered according to the sizes of their eigenvalues, strongest first.

The output powers in the kth channel, k=1,2, due to the jth signal, j=1,2, were computed from

$$P_{j(k)} = P_j |\tilde{e}_k^H \tilde{g}_j|^2 \qquad (34)$$

The corresponding noise power in each of the output channels was given by σ^2.

The output channel favouring the communications signal was selected for evaluation purposes. This was usually the second channel, as the communications power was normally less than the jamming power.

Figure 1a shows the computed ideal performance of the eigenvector separation technique, for the case of a two-element half-wavelength-spaced array and a normally incident communications signal. The output signal to noise-plus-interference ratio SNIR(out) is plotted as a function of jamming incidence angle for various values of SNIR(in). Two sets of curves are shown: one for negligible noise power (-100dB relative to communications) and the other, for a plausible noise power (-30dB).

With negligible input noise power, when the jamming incidence angle is close to that of the communications (0°), the performance equals that of power ratio inversion. (A singular point for which SNIR(out) is undefined occurs when the angles are exactly equal; this is not shown on the figures.) When the jamming angle approaches either + or - 90°, SNIR(out) becomes infinite, suggesting perfect separation. The response vector of the array to the jamming is orthogonal to the communications response vector for these directions. At intermediate angles, performance lies between that of perfect separation and power ratio inversion. It is interesting to note, that even with near-equal power levels (SNIR(in) = -1 and -3dB in Figure 1a), acceptable performance (taken as SNIR(out) > 10dB) is achieved for a significant fraction of jammer incidence angles.

The addition of input noise, as illustrated in Figure 1a, causes the performance to drop at nearly-

Figure 1a. SNIR(out) as a function of jamming incidence angle, for a normally incident communications signal and various values of SNIR(in) on a λ/2-spaced 2-element array using eigenvector weighting. Curves are shown for negligible input noise power (-100dB relative to communications) and plausible input noise power (-30dB).

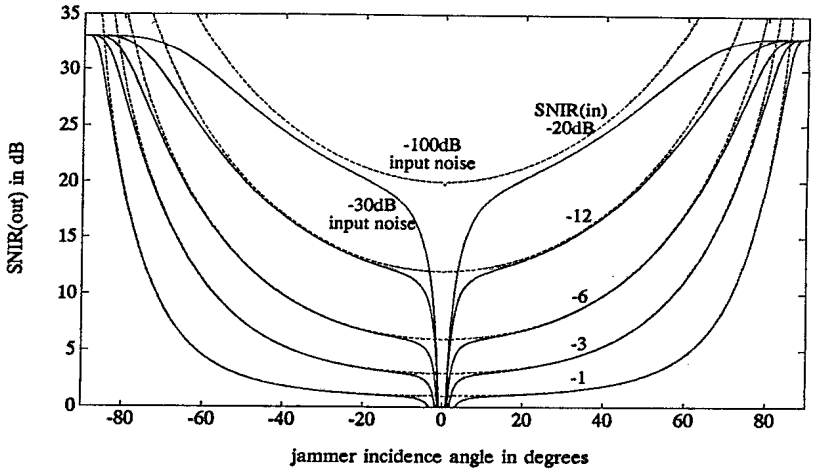

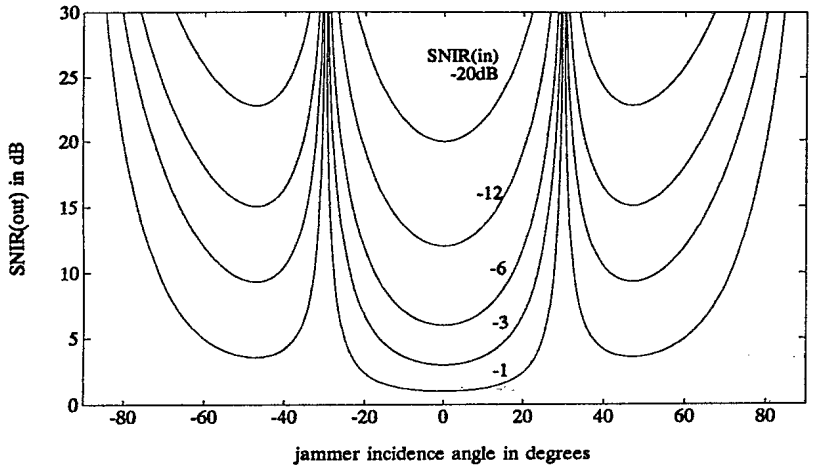

Figure 1b. SNIR(out) as a function of jamming incidence angle, for a normally incident communications signal and various values of SNIR(in) on a λ/2-spaced 4-element linear array using eigenvector weighting. Input noise power was negligible (-100dB relative to communications).

Figure 1c. SNIR(out) as a function of jamming incidence angle, for a normally incident communications signal and various values of SNIR(in) on a λ/2-spaced 8-element linear array using eigenvector weighting. Input noise power was negligible (-100dB).

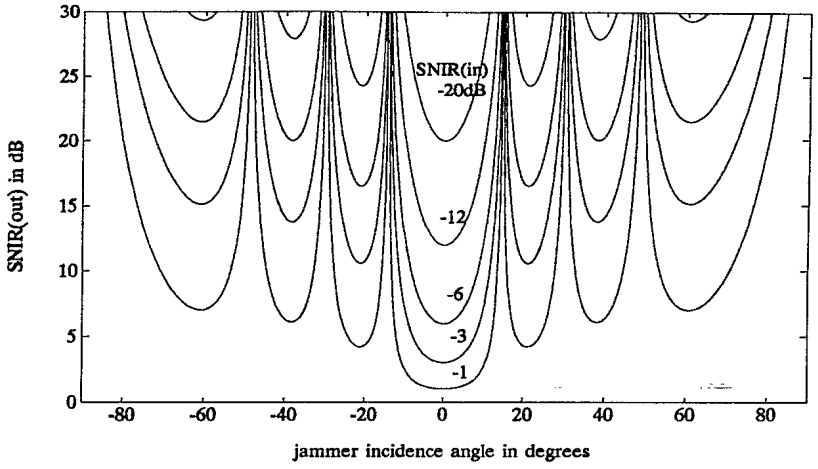

equal signal directions. This happens because the output communications power approaches zero when its direction approaches that of the stronger jamming signal, while the output noise power remains finite. This is a feature of most interference-cancelling techniques, not only eigenvector weighting. The addition of noise also limits the maximum value of SNIR(out) which is achieved at directions where the input signals are orthogonal, to the input signal plus noise ratio SNR(in) (30dB) plus the array gain (3dB). Apart from these limitations, the observations noted

for the noise-absent case are true for the noise-present case.

In the remainder of the modelling results discussed, a negligible noise power (-100dB) has been used. This is done in order to simplify the results so that other features are clearer. The addition of noise does not alter the conclusions thus obtained.

Figures 1b and 1c show the corresponding performances for a four and eight-element linear half-wavelength spaced array, respectively. Like the two-element case, the performance drops to that of power ratio inversion when the jamming angle approaches that of the communications, and increases to that of perfect signal separation, at jamming angles corresponding to orthogonal jamming and communications response vectors. The performances for near-equal input power levels (SNIR(in) = -1, -3dB) are seen to be acceptable (SNIR(out) > 10dB) over a wider range of jamming angles, as the number of elements increases.

Figures 2a, b, and c show corresponding three-dimensional plots for the case of SNIR(in) = -3dB, for the two, four, and eight-element half-wavelength spaced array respectively. SNIR(out) is plotted as a function of the jamming and communications incidence angle, in this case. The plot extends over all jamming and communications incidence angles, -90 to +90°, relative to the array. Provided that the angles lie near the horizon, the incidence angles represent equally likely azimuth angles. In order to provide a measure of the fraction of cases for which communications is acceptable, the plots are truncated at the SNIR(out) = 10dB level. The fraction of angles for which SNIR(out) > 10dB is thus illustrated. As previously suggested by figures 1a, b, and c, acceptable communications is achieved for near-equal input powers over a wider fraction of angles, as the number of elements increases.

The modelling represented by Figures 2a, b, and c was repeated for other values of SNIR(in), to

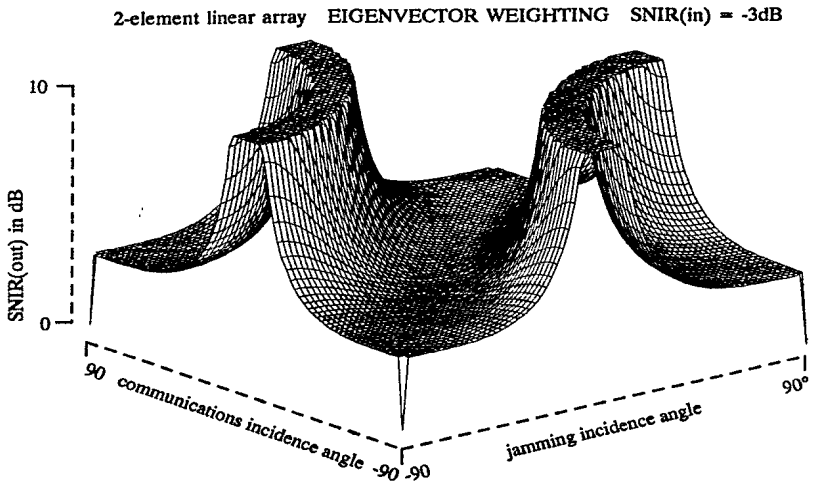

Figure 2a. Three-dimensional plot of SNIR(out) as a function on communications and jamming incidence angle, for input communications, jamming and noise signals of 0, 3, and -100dB respectively, on a λ/2-spaced 2-element array using eigenvector weighting. The plot is limited above at 10dB.

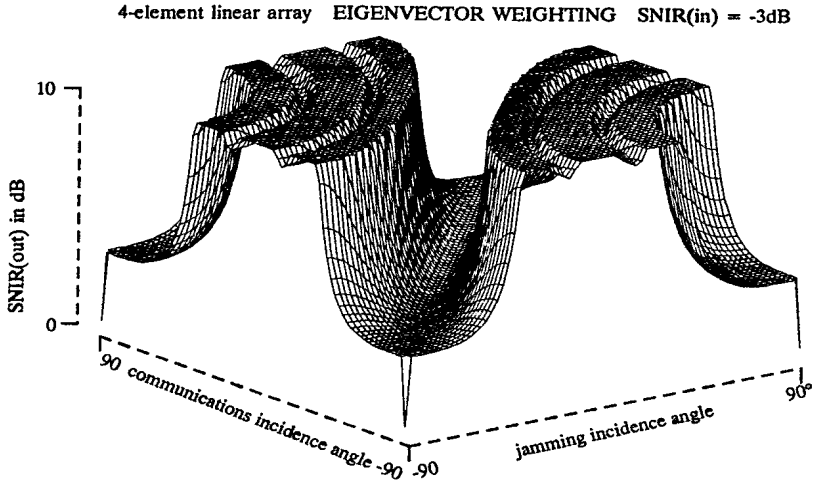

Figure 2b. Three-dimensional plot of SNIR(out) as a function on communications and jamming incidence angle, for input communications, jamming and noise signals of 0, 3, and -100dB respectively, on a λ/2-spaced 4-element linear array using eigenvector weighting. The plot is limited above at 10dB.

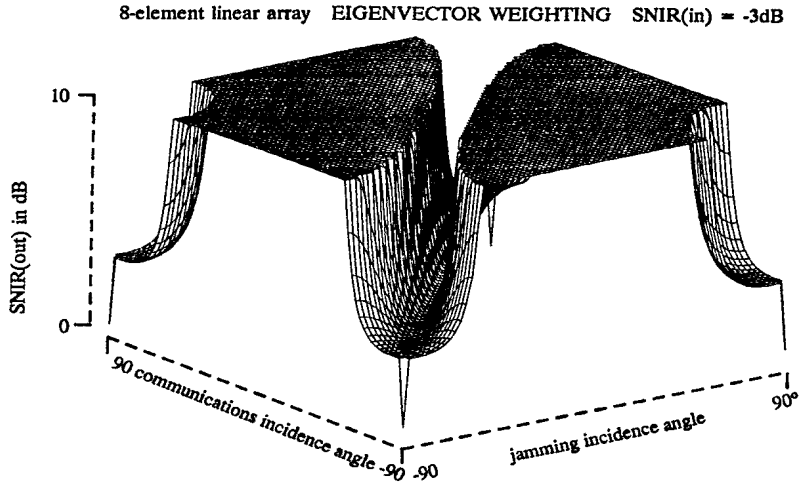

Figure 2c. Three-dimensional plot of SNIR(out) as a function on communications and jamming incidence angle, for input communications, jamming and noise signals of 0, 3, and -100dB respectively, on a λ/2-spaced 8-element linear array using eigenvector weighting. The plot is limited above at 10dB.

determine the extent to which acceptable communications can be achieved with eigenvector weighting, at near-equal signal levels. The fraction of angles, for which acceptable communications (SNIR(out) > 10dB) is achieved, is plotted for the two, four and eight-element linear arrays as a function of SNIR(in) in Figure 3. This fraction is seen to be symmetric about SNIR(in) = 0°. This result arises from the performance symmetry in the two-signal case, described in equation 30 in terms of the relative output powers being inverted between the two signal output channels. The improvement in performance with increasing number of elements is also evident. To put these results in perspective, it should be noted that the power-inversion techniques would not result in acceptable communications at these values of SNIR(in), for any angles. While not a completely satisfactory solution for the case of

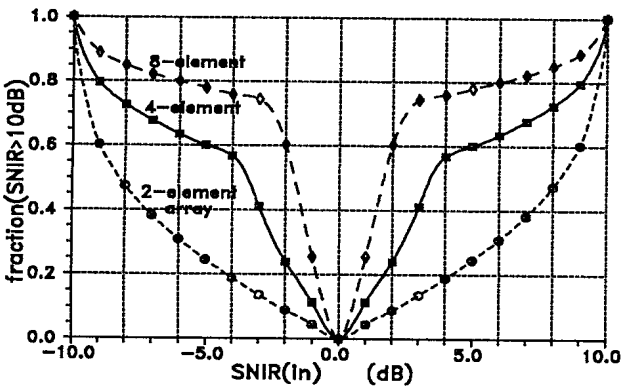

Figure 3. Fraction of communications and jamming directions for which SNIR(out) exceeds 10dB, as a function of SNIR(in), for 2, 4, and 8-element l/2-spaced linear arrays using eigenvector weighting.

near-equal powers, Figure 3 shows that eigenvector separation can provide acceptable performance in a large fraction of cases, and thus is substantially better than the power-inverting alternatives.

The effect of gain differences in the input channels is illustrated in Figures 4a and b. These figures demonstrate the effects of reducing the gain in one channel, relative to the others, for the two and four-element linear half-wavelength arrays. The communications signal was normally incident and SNIR(in) was -3dB, with a negligible noise level. SNIR(out) was plotted as a function of jamming incidence angle, for various channel gain mismatches. It can be seen that the array performance for those directions where eigenvector separation performs best deteriorates rapidly with channel gain differences. This effect is worst for the two element case; for very large gain differences, the 2-element performance is everywhere reduced to that of power ratio inversion. For the four-element case the behavior is more complex, and depends on which and how many elements have reduced gain. The example shown in Figure 4b is for a single attenuated channel. When three of the four channels are severely attenuated, the performance was also found to be reduced to that of power ratio inversion. These results indicate that efforts should be made to provide equal input channel gains for systems where the eigenvector separation technique is used.

The superior performance of the eigenvector technique over power ratio inversion methods was shown analytically for the case of two signals and identical element patterns. On an intuitive basis, the increased degrees of freedom used in determining the weights for the first and second output channels suggest that the eigenvector technique is likely to be

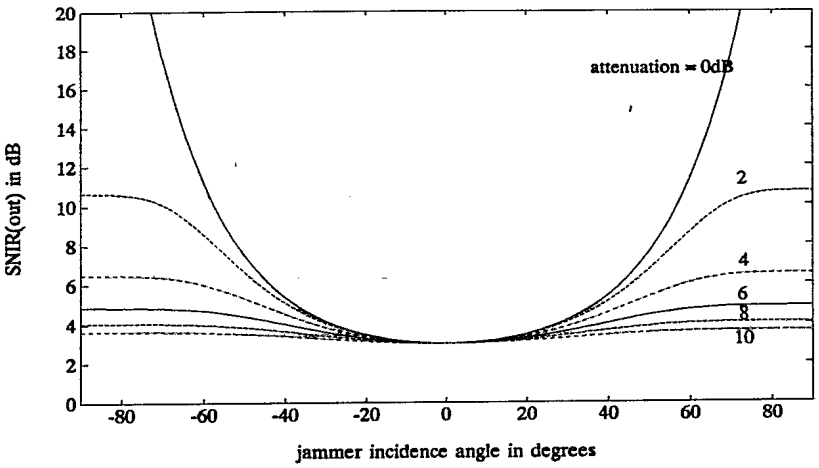

Figure 4a. Effect of channel gain differences on eigenvector weighting performance of a λ/2-spaced 2-element array, for a normally incident communications signal and communications, jamming, and noise powers of 0, 3, and -100dB, and various values of attenuation applied to one of the channels.

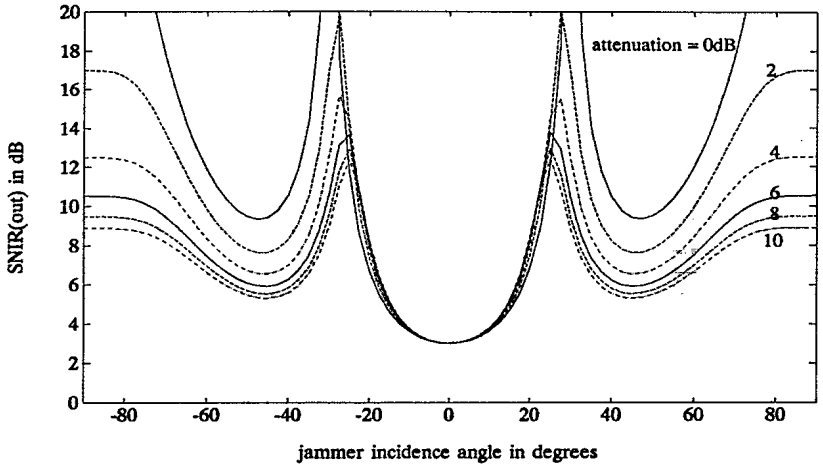

Figure 4b. Effect of channel gain differences on eigenvector weighting performance of a λ/2-spaced 2-element linear array, for a normally incident communications signal and communications, jamming, and noise powers of 0, 3, and -100dB, and various values of attenuation applied to one of the channels.

superior to power ratio inversion (as demonstrated by Gram-Schmidt orthogonalization which fixes the first weight vector and permits only one degree of freedom in the second weight vector) much more often than not.

A plausible example of non-identical element patterns is provided in the four-element square array with differently-directed offset-circular element patterns, illustrated in Figure 5. The performance for this array using a front-to-back ratio of 10dB in the element patterns, for SNIR(in) = -3dB, is illustrated in Figure 6. In this figure, SNIR(out) is plotted versus jamming and communications incidence angles in a 3-dimensional format. As can be seen in this figure, the array performance has a minimum of SNIR(out) = 3dB, which occurs when the jamming incidence angle approaches that of the communications. Substantially better performances are achieved for a large fraction of possible

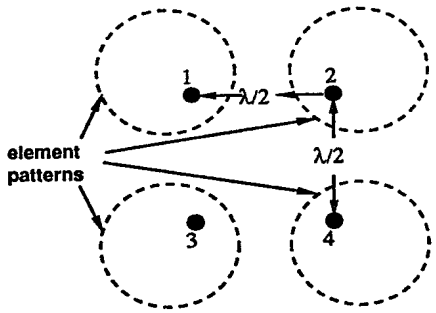

Figure 5. Modelled square array with differently-directed offset-circle element patterns.

directions. Thus the eigenvector performance with this array is better than that of a similar array with non-directive elements using power-ratio inverting techniques.

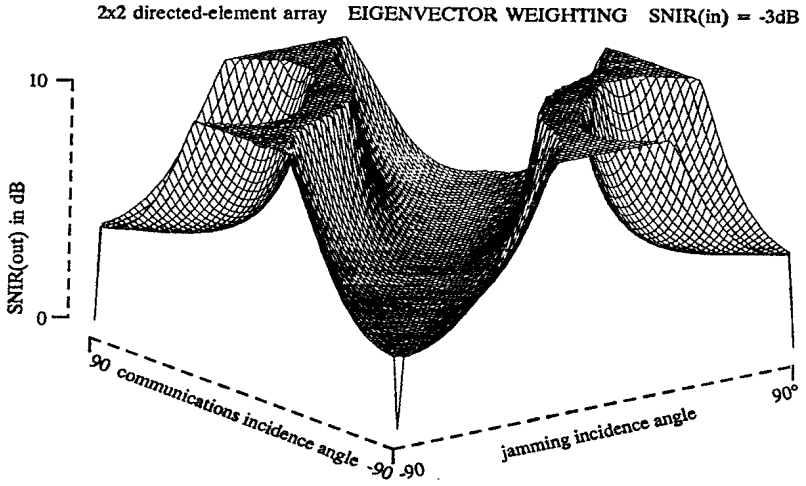

Figure 6. Three-dimensional plot of SNIR(out) obtained with eigenvector weighting, as a function of communications and jamming incidence angles, for input communications, jamming, and noise signals of 0, 3, and -100dB respectively, for the array of Figure 5 with a forward to back ratio of 10dB in the element patterns. The plot is limited above at 10 dB.

Further, since the signals which are weighted and combined in any adaptive array technique are those seen by the element antennas, the effect of directive elements on power-ratio inversion methods is expected to be merely a shift in the value of SNIR(in) corresponding to a certain value of SNIR(out). For any given set of signal directions, the poor values of SNIR(out) corresponding to near-equal input powers (as seen by the antennas) would still occur under power ratio inversion.

From the above, it can be inferred that in situations where a single algorithm is to be used to cover a range of possible signal powers and directions, the eigenvector technique is preferred whether the array elements are differently directed or not. However, if the implementation is such that different algorithms can be tried on a case-by-case basis, then including a power ratio inversion technique along with eigenvector weighting will at times improve performance, if the array elements are differently directed.

SIMULATION

The ideal covariance matrix **R** assumed in the analysis and used to obtain the modelling results reported herein differs from the time-average estimate found in practice, in that the estimation errors due to the finite averaging period and random signal variations have not contributed to the covariance matrix elements. These errors give rise to small apparent correlations between the two independent signals and the noise signals. As a check on the practical applicability of the analysis and the reliability of the modelling studies, a more detailed simulation was carried out for the two and four-element arrays.

The simulations included a binary-phase-coded communications signal plus a single jamming signal, incident on half-wavelength spaced linear arrays. The jamming signal was either pure-tone or white noise. The input signals were constructed on a sample-by sample basis, using a sample rate of 5 samples/bit. Noise values and white-noise jamming values were assumed to be independent between samples. From each block of 64 input samples, a block covariance matrix was formed. A weighted average was taken between the block covariance matrix and the previous covariance matrix estimate, in order to form a new covariance matrix estimate. The time constant of the weighted averaging was 2.54 blocks. The simulation was run for 32 blocks, and from the weights thus obtained for each block, SNIR(out) found, on a block-by-block basis.

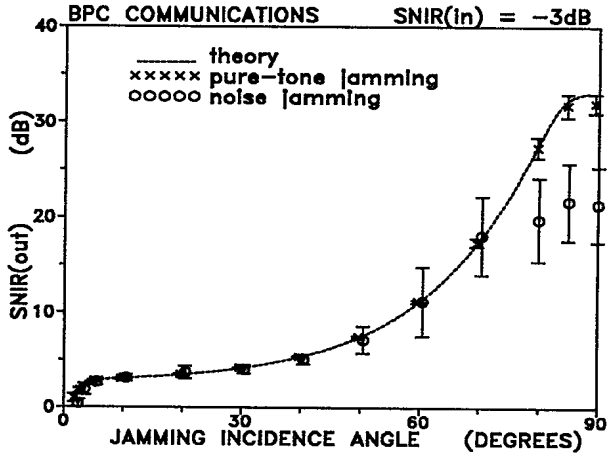

Figure 7a. Theoretical and simulated performance of a λ/2-spaced 2-element array with eigenvector weighting, in the presence of a normally-incident 0dB communications signal, a 3dB jamming signal, and -30dB input noise. Mean values and rms deviations are shown for pure-tone and noise jamming simulations.

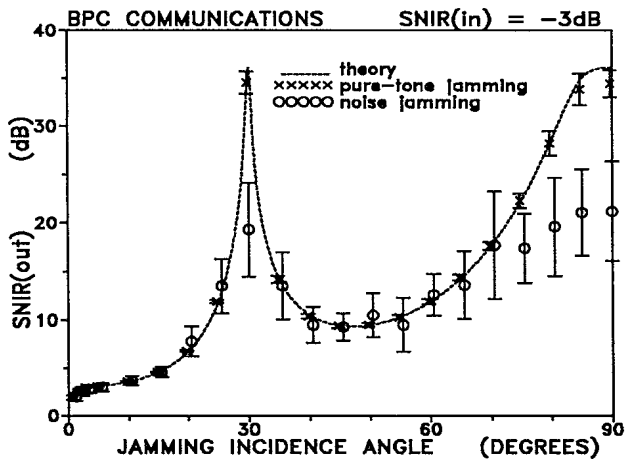

Figure 7b. Theoretical and simulated performance of a λ/2-spaced 4-element linear array with eigenvector weighting, in the presence of a normally-incident 0dB communications signal, a 3dB jamming signal, and -30dB input noise. Mean values and rms deviations are shown for pure-tone and noise jamming simulations.

Figures 7a and b show the simulation performance, for 3dB input jamming power and -30dB noise power, relative to the input communications power, for the two and four-element arrays respectively. SNIR(out) is plotted as a function of the jamming incidence angle, for a normally incident communications signal. Average values and rms deviations (on the block-by-block results) are plotted for the cases of pure-tone and white-noise jamming. Also shown are the theoretical statistics-independent curves, computed from the previous modelling program, for these input power levels.

The pure-tone jamming results agree well with the theoretical curves for both the two and four-element arrays, implying that the random binary-phase coding of the communications does not substantially affect performance. The noise jamming results are in agreement with the theoretical curves, at values of SNIR(out) up to 15dB. At higher valuesof SNIR(out), the random nature of the noise jamming causes the average performance to be reduced below that of the theoretical curve. Also, the block-to-block rms variation in performance is greater for the noise jamming, and for higher values of SNIR(out). It should be noted that the reduction in performance below the theoretically expected value, found for the case of noise jamming, does not extend down to the minimum values of SNIR (approx. 10dB) needed for acceptable communications.

The simulation results support the validity of the conclusions drawn from the analysis and the ideal modelling studies, for practical applications.

REFERENCES

[1] R.T. Compton, Jr., "The Power-Inversion Adaptive Array: Concept and Performance", IEEE Trans. Aerospace Electron. Syst., Vol. AES-15, pp. 803-814, 1979

[2] K. Gerlach and F. Kretschmer, Jr., "Convergence Properties of Gram-Schmidt and SMI Adaptive Algorithms", IEEE Trans. Aerospace Electron. Syst., Vol. AES-26, pp. 44-56, 1990

[3] C.M. Hackett, Jr., " Adaptive Arrays Can Be Used to Separate Communication Signals", IEEE Trans. Aerospace Electron. Syst., Vol. AES-17, pp. 234-247, 1981.

[4] R. Spohn, V. Frost, R. Balasubramaniam, R. Moats, "Development of an Eigenvector Sorting Algorithm for HF Antenna Arrays", RADC-TR-88-68 Final Technical Report, University of Kansas, 1988

[5] S. Haykin,"Adaptive Filter Theory ", Ch. 2, Prentice-Hall, 1986

[6] R.W. Jenkins and K.W. Moreland, "A Comparison of the Eigenvector Separation and Gram-Schmidt Adaptive Antenna Techniques", submitted for publication, 1990

APPENDIX

It is proven here that, given isotropic array elements,

$$|\tilde{e}_1^H \tilde{g}_1| \geq |\tilde{e}_1^H \tilde{g}_2| \qquad (33)$$

In equation 12, the covariance matrix $\mathbf{R}$ is written as $\mathbf{R} = \mathbf{S} + \mathbf{N}$, where $\mathbf{S} = \mathbf{GPG}^H$ and $\mathbf{N} = \sigma^2\mathbf{I}$ are the signal and noise contributions respectively. The eigenvectors $\tilde{e}_1$, $\tilde{e}_2$ of $\mathbf{R}$ were shown to be also eigenvectors of the n x n matrix $\mathbf{S}$. To show (33) is true, it is helpful to find $\tilde{e}_1$ by solving the eigenvector equation of $\mathbf{S}$. Using the factorization

$$\mathbf{S} = (\mathbf{G}\sqrt{\mathbf{P}})(\mathbf{G}\sqrt{\mathbf{P}})^H, \qquad (A1)$$

where $\sqrt{\mathbf{P}} = \begin{bmatrix} \sqrt{P_1} & 0 \\ 0 & \sqrt{P_2} \end{bmatrix}$ and $\mathbf{G} = [\tilde{g}_1, \tilde{g}_2]$,

the eigenvector equation of $\mathbf{S}$ can be expressed as

$$(\mathbf{G}\sqrt{\mathbf{P}})(\mathbf{G}\sqrt{\mathbf{P}})^H \tilde{e}_k = \gamma_k \tilde{e}_k \qquad (A2)$$

Premultiplying (A2) by $(\mathbf{G}\sqrt{\mathbf{P}})^H$ yields the simpler 2-dimensional eigenvector equation

$$\mathbf{T}\tilde{v}_k = \gamma_k \tilde{v}_k , \qquad (A3)$$

where

$$\tilde{v}_k = (\mathbf{G}\sqrt{\mathbf{P}})^H \tilde{e}_k \qquad (A4)$$

and

$$\mathbf{T} = (\mathbf{G}\sqrt{\mathbf{P}})^H(\mathbf{G}\sqrt{\mathbf{P}}) \qquad (A5)$$

$\mathbf{T}$ is a 2 x 2 matrix whose eigenvalues are the eigenvalues γ_k of $\mathbf{S}$, and whose eigenvectors are given by $\tilde{v}_k$. The eigenvector $\tilde{e}_k$ of $\mathbf{S}$ can be found in terms of $\tilde{v}_k$ by using (A4) to replace the factor $(\mathbf{G}\sqrt{\mathbf{P}})^H\tilde{e}_k$ on the right-hand side of (A2) by $\tilde{v}_k$, thus obtaining

$$\tilde{e}_k = \frac{1}{\gamma_k}(\mathbf{G}\sqrt{\mathbf{P}})\tilde{v}_k.$$

The eigenvector scale factor $\frac{1}{\gamma_k}$ is arbitrary and can be dropped, so that

$$\tilde{e}_k = (\mathbf{G}\sqrt{\mathbf{P}})\,\tilde{v}_k \qquad (A6)$$

Proceeding now to find the eigenvectors $\tilde{v}_k$ of $\mathbf{T}$, $\mathbf{T}$ is expanded in terms of its elements using (A1) and (A5) to obtain:

$$\mathbf{T} = \begin{bmatrix} P_1|\tilde{g}_1|^2 & \sqrt{P_1P_2}\,\tilde{g}_1^H\tilde{g}_2 \\ \sqrt{P_1P_2}\,\tilde{g}_2^H\tilde{g}_1 & P_2|\tilde{g}_2|^2 \end{bmatrix} \qquad (A7)$$

The quadratic equation $\det(\mathbf{T} - \gamma\mathbf{I}) = 0$ is solved for the eigenvalues of $\mathbf{T}$, obtaining

$$\gamma_{1,2} = \frac{P_1|\tilde{g}_1|^2+P_2|\tilde{g}_2|^2}{2} \pm \sqrt{P_1P_2}\,|\tilde{g}_1^H\tilde{g}_2|\sqrt{1+\chi^2} \qquad (A8)$$

$$\text{where } \chi = \frac{P_2|\tilde{g}_2|^2-P_1|\tilde{g}_1|^2}{2\sqrt{P_1P_2}\,|\tilde{g}_1^H\tilde{g}_2|} \qquad (A9)$$

γ_1 corresponds to the plus sign in (A8) since it is the larger eigenvalue by the ordering convention used. Setting

$$e^{j\beta} = \frac{\tilde{g}_1^H\tilde{g}_2}{|\tilde{g}_1^H\tilde{g}_2|} \quad \text{and} \quad \mu = \chi + \sqrt{1+\chi^2}, \qquad (A10)$$

$\tilde{v}_1$ is given by

$$\tilde{v}_1 = \begin{bmatrix} 1 \\ \mu e^{-j\beta} \end{bmatrix} \qquad (A11)$$

Substituting (A10) and (A11) in (A6), $\tilde{e}_1$ is found to be

$$\tilde{e}_1 = (\mathbf{G}\sqrt{\mathbf{P}})\,\tilde{v}_1 = \sqrt{P_1}\,\tilde{g}_1 + \sqrt{P_2}\,\mu e^{-j\beta}\,\tilde{g}_2 \qquad (A12)$$

and

$$|\tilde{e}_1^H\tilde{g}_1| = |\tilde{g}_1|^2(\sqrt{P_1} + \xi\mu\sqrt{P_2}), \qquad (A13)$$

$$\text{where } \xi = \frac{|\tilde{g}_1^H\tilde{g}_2|}{|\tilde{g}_1|^2}. \qquad (A14)$$

Similarly,

$$|\tilde{e}_1^H\tilde{g}_2| = |\tilde{g}_1|^2(\xi\sqrt{P_1} + \mu\sqrt{P_2}) \qquad (A15)$$

The array elements are assumed to have isotropic gains. Therefore, $\tilde{g}_k$ is of the form

$$[\rho_1 e^{j\delta 1k}, \rho_2 e^{j\delta 2k}, \text{- -}, \rho_n e^{j\delta nk}]^T,$$

implying that

$$|\tilde{g}_1| = |\tilde{g}_2| = (\textstyle\sum_{i=1}^{n} \rho_i^2)^{1/2} \qquad (A16)$$

From (A15), (A16) and the Cauchy-Schwartz inequality,

$$\xi = \frac{|\tilde{g}_1^H\tilde{g}_2|}{|\tilde{g}_1|^2} \le \frac{|\tilde{g}_1||\tilde{g}_2|}{|\tilde{g}_1|^2} = 1, \text{ which implies that}$$

$$0 \le \xi \le 1 \qquad (A17)$$

From (A9), the input power ordering ($P_1 \ge P_2$), and isotropy ($|\tilde{g}_1| = |\tilde{g}_2|$), χ is non-positive. Applying this to (A10), μ is seen to lie in the range

$$0 \le \mu \le 1 \qquad (A18)$$

From (A15), (A16), (A17) and (A18), together with the input power ordering, it can be shown that

$$|\tilde{e}_1^H\tilde{g}_1| - |\tilde{e}_1^H\tilde{g}_2| = |\tilde{g}_1|^2(1-\xi)(\sqrt{P_1} - \mu\sqrt{P_2}) \ge 0 \qquad (A19)$$

Therefore, $|\tilde{e}_1^H\tilde{g}_1| \ge |\tilde{e}_1^H\tilde{g}_2|$, which proves that the eigenvector technique provides better signal separation than the power ratio inversion techniques under the condition of isotropic element patterns. When the signals are close in direction, then ξ approaches unity (A14), thus causing $|\tilde{e}_1^H\tilde{g}_1|$ to approach $|\tilde{e}_1^H\tilde{g}_2|$ (A19). Therefore, power ratio inversion provides a greatest lower bound to the eigenvector separation performance, given the isotropy condition.

DISCUSSION

George H. HAGN

What is the impact of coherent multipath on the method you have presented ?

Have you gone beyond the theorefical stage which you presented to us to build a practical system ?

AUTHOR'S REPLY

If the multipath is completely coherent, then the resultant signal from that source will have a certain time-independent phase relationship between antenna elements. The technique will deal with it as it would any simple-mode signal, and performance would not be reduced. If coherence is partial however, a deterioration in performance might result.

We have a test bed for HF and VHF applications, part of which is a programmable real-time processing system. The eigen vector method will be implemented on that test bed, in 2-element form, in the near future, and, in 4-element form, about a year from now.